Structure and Promoter Activity of an Islet-Specific Glucose-6-Phosphatase Catalytic Subunit–Related Gene

Daniel H. Ebert, Larry J. Bischof, Ryan S. Streeper, Stacey C. Chapman, Christina A. Svitek, Joshua K. Goldman, Clayton E. Mathews, Edward H. Leiter, John C. Hutton, and Richard M. O'Brien

In liver and kidney, the terminal step in the gluconeogenic pathway is catalyzed by glucose-6-phosphatase (G-6-Pase). This enzyme is actually a multicomponent system, the catalytic subunit of which was recently cloned. Numerous reports have also described the presence of G-6-Pase activity in islets, although the role of G-6-Pase in this tissue is unclear. Arden and associates have described the cloning of a novel cDNA that encodes an islet-specific G-6-Pase catalytic subunit–related protein (IGRP) (Arden SD, Zahn T, Steegers S, Webb S, Bergman B, O'Brien RM, Hutton JC: Molecular cloning of a pancreatic islet–specific glucose-6-phosphatase catalytic subunit related protein (IGRP). *Diabetes* 48:531–542, 1999). We screened a mouse BAC library with this cDNA to isolate the IGRP gene, which spans ~8 kbp of genomic DNA. The exon/intron structure of the IGRP gene has been mapped and, as with the gene encoding the liver/kidney G-6-Pase catalytic subunit, it is composed of five exons. The sizes of these exons are 254 (I), 110 (II), 112 (III), 116 (IV), and 1284 (V) bp, similar to those of the G-6-Pase catalytic subunit gene. Two interspecific backcross DNA mapping panels were used to unambiguously localize the IGRP gene (map symbol *G6pc-rs*) to the proximal portion of mouse chromosome 2. The IGRP gene transcription start site was mapped by primer extension analysis, and the activity of the IGRP gene promoter was analyzed in both the islet-derived HIT cell line and the liver-derived HepG2 cell line. The IGRP and G-6-Pase catalytic subunit gene promoters show a reciprocal pattern of activity, with the IGRP promoter being ~150-fold more active than the G-6-Pase promoter in HIT cells. *Diabetes* 48:543–551, 1999

From the Department of Molecular Physiology and Biophysics (D.H.E., L.J.B., R.S.S., S.C.C., C.A.S., J.K.G., R.M.O.), Vanderbilt University Medical School, Nashville, Tennessee; the Jackson Laboratory (C.E.M., E.H.L.), Bar Harbor, Maine; and the Barbara Davis Center for Childhood Diabetes (J.C.H.), University of Colorado Health Sciences Center, Denver, Colorado.

Address correspondence and reprint requests to Richard M. O'Brien, Department of Molecular Physiology and Biophysics, 761 MRB II, Vanderbilt University Medical School, Nashville, TN 37232-0615. E-mail: richard.obrien@mcmail.vanderbilt.edu.

Received for publication 23 July 1998 and accepted in revised form 30 November 1998.

R.M.O. is a paid consultant for Oncogene Science.

CAT, chloramphenicol acetyltransferase; DMEM, Dulbecco's modified Eagle's medium; G-6-Pase, glucose-6-phosphatase; GSD, glycogen storage disease; HGP, hepatic glucose production; HNF, hepatocyte nuclear factor; IGRP, islet-specific glucose-6-phosphatase catalytic subunit–related protein; IRS, insulin response sequence; MODY, maturity-onset diabetes of the young; PCR, polymerase chain reaction; RT-PCR, reverse transcription–polymerase chain reaction; SSC, sodium chloride/sodium citrate.

Glucose-6-phosphatase (G-6-Pase) catalyses the hydrolysis of glucose-6-phosphate, the terminal step in the gluconeogenic and glycogenolytic pathways, allowing for the release of glucose into the bloodstream (1). The same reaction is catalyzed by G-6-Pase in liver and kidney, although the relative contribution of each tissue in providing glucose for the brain during periods of fasting is the subject of continuing debate (1,2). G-6-Pase is thought to exist as a multicomponent, integral membrane system located in the endoplasmic reticulum (3–5). Several components of the G-6-Pase system have recently been cloned, including the G-6-Pase catalytic subunit (6,7), the putative glucose-6-phosphate transporter (8), and the putative glucose transporter (GLUT7) (9).

Type 2 diabetes is characterized by defects in insulin secretion, insulin-dependent peripheral glucose utilization, and hepatic glucose production (HGP) (10). As a consequence of insulin resistance, the ability of insulin to stimulate peripheral glucose utilization and repress HGP in patients with type 2 diabetes is reduced (10). The elevated HGP is due to an increased rate of gluconeogenesis, rather than glycogenolysis (11,12). Insulin normally inhibits G-6-Pase catalytic subunit gene transcription (13–15), and various investigators have speculated that overexpression of the G-6-Pase catalytic subunit, as a consequence of insulin resistance, may contribute to the increased HGP in type 2 diabetes (16–19). Indeed, in animal models of both type 1 (20–24) and type 2 (25) diabetes, hepatic G-6-Pase activity (20,21,23,24) and G-6-Pase catalytic subunit mRNA levels (21–25) are increased, potentially explaining, in part, the elevated HGP (18).

The causes of the defect in insulin secretion in type 2 diabetes are unclear (26,27), but in maturity-onset diabetes of the young (MODY), a rare form of type 2 diabetes, aberrant insulin secretion can arise because of mutations in several genes. Thus, distinct subtypes of MODY can be ascribed to mutations in the genes encoding HNF-4 (MODY1), glucokinase (MODY2), HNF-1 α (MODY3), IPF-1 (MODY4), and HNF-1 β (MODY5) (28–32). The bases for aberrant insulin secretion in MODY1, 3, 4, and 5 are unclear and are probably complex, since, in each case, the mutated gene encodes a transcription factor that is likely to regulate the expression of multiple islet genes. By contrast, the pathophysiology of MODY2 is well understood, since glucokinase is a key element in glucose sensing by the β cell, coupling the rate of islet glucose

metabolism, and thus insulin secretion, to the circulating concentration of glucose (33).

As reviewed in the studies by Arden et al. (34) and Foster et al. (5), the majority of studies have found that G-6-Pase activity is detected in islets but at a lower level than found in liver. Using reverse transcription–polymerase chain reaction (RT-PCR), Tokuyama et al. (35) showed that the gene encoding the G-6-Pase catalytic subunit is expressed in normal rat islets and that expression is increased in islets isolated from both prediabetic and diabetic Zucker diabetic fatty (ZDF) rats. In addition, G-6-Pase activity is elevated in islets isolated from *ob*/*ob* mice, leading to increased glucose cycling and reduced glucose-stimulated insulin secretion (36,37). Clearly, overexpression of G-6-Pase in islets would uncouple glucose-stimulated insulin secretion. Thus the overexpression of a single gene could contribute to two of the characteristic defects in type 2 diabetes, increased HGP and impaired glucose-stimulated insulin secretion.

Although the gene encoding the G-6-Pase catalytic subunit is expressed in rat islets (35), the islet enzyme displays distinct kinetic behavior compared with that assayed in hepatic extracts (34). Furthermore, antibodies raised to the G-6-Pase catalytic subunit do not consistently detect a specific complex when used in Western blotting experiments with INS-1 cell extracts (38). These observations might be explained by the existence of a distinct G-6-Pase catalytic subunit isoform in islets. In their article, Arden et al. (34) describe the identification of a novel islet-specific cDNA that encodes a protein, designated IGRP, that is highly homologous to the G-6-Pase catalytic subunit, although its actual catalytic activity is unknown. In this article, we describe the cloning of the IGRP gene. A comparison of the exon/intron structures of the G-6-Pase catalytic subunit and the IGRP genes show that they are highly conserved, supporting the hypothesis that they are evolutionarily related. By contrast, the G-6-Pase catalytic subunit and IGRP gene promoters show highly selective activity in liver and islet cell lines, respectively.

RESEARCH DESIGN AND METHODS

Materials. [α-^{32}P]dATP (>3,000 Ci/mmol) and [γ-^{32}P]dATP (>5,000 Ci/mmol) were obtained from Amersham; [^{3}H]acetic acid, sodium salt (>10 Ci/mmol) was purchased from ICN. The mouse BAC library, from which the IGRP gene was isolated (see below), was obtained from Genome Systems (St. Louis, MO).

General cloning, DNA isolation, and sequencing procedures. Plasmid DNA purification, subcloning, and restriction nuclease analysis were performed as described (39). DNA fragments used for subcloning and labeling were isolated from agarose gels using the Qiaex II gel extraction kit (Qiagen, Valencia, CA). Zeta-probe membranes (Bio Rad, Hercules, CA) were used for DNA hybridization analysis, and both alkaline transfer and hybridization using the standard protocol were performed according to the manufacturer's instructions. DNA probes were labeled by random oligonucleotide priming in the presence of [α-^{32}P]dATP using the Stratagene (La Jolla, CA) Prime-It II random primer labeling kit according to the manufacturer's instructions. The specific activity of the various probes used ranged from ~0.2 to ~1.2 Ci/nmol. DNA sequencing was performed using the USB Sequenase kit. All DNA sequences are numbered relative to the experimentally determined transcription start site, designated +1 (Fig. 3).

Isolation of IGRP genomic clones. The Genome Systems mouse BAC library was screened, according to the manufacturer's instructions, using the full-length IGRP cDNA, designated 1B1 (34), as the labeled probe. Briefly, the five BAC library filters were incubated overnight in 200 ml hybridization solution that contained 6× sodium chloride/sodium citrate (SSC), 0.5% SDS, 100 µg/ml salmon sperm DNA, and 100 ng labeled probe (~500,000 dpm/ml). The filters were washed five times, according to the manufacturer's instructions, and exposed for ~2 h at –80°C to Kodak XAR film. The location of specific hybridization signals, identified as double dots on the autoradiograph, was determined from the filter map provided, and the relevant BAC clone was then purchased from Genome Systems. The large-scale isolation of BAC plasmid DNA was then performed as recommended by the manufacturer.

Characterization of IGRP genomic clones. One recombinant BAC plasmid, designated BAC IGRP-3, contained the entire IGRP gene (Fig. 1). BAC IGRP-3 plasmid DNA was digested with a panel of restriction enzymes, and DNA hybridization analysis was performed using labeled fragments representing either the 5′ or 3′ end of the 1B1 IGRP cDNA (34). These 5′ or 3′ 1B1 IGRP cDNA fragments were isolated from the pSV.SPORT1 1B1 clone (34) (Life Technologies, Grand Island, NY) by digestion with *Sal*I and *Pvu*II or *Xmn*I and *Not*I, respectively. Genomic DNA fragments that hybridized to these labeled probes were then subcloned into the pGEM7 plasmid vector (Promega) for sequence analysis.

Digestion of the BAC IGRP-3 plasmid with *Xba*I generated multiple fragments (Fig. 1). The arrangement of these fragments in the BAC IGRP-3 plasmid and the identification of the exon/intron boundaries was determined by direct DNA sequencing of both DNA strands and comparison with the IGRP cDNA sequence (34). The sizes of the four introns in the IGRP gene (Fig. 1) were calculated by direct sequencing (intron D) or estimated by PCR (introns A, B, C). In the latter case, the size of each intron was estimated using two separate primer pairs, and in each case the difference in the size of the PCR products was as expected. PCR was performed according to the following protocol: the final reaction volume (100 µl) contained 100 pmol of each primer; either 1× Vent DNA polymerase buffer (New England Biolabs, Beverly, MA) or 1× PCR Buffer (Perkin Elmer, Foster City, CA); 0.2 mmol/l dATP, dCTP, dGTP, and dTTP; 20 ng BAC IGRP-3 plasmid DNA; and either 2 U Vent DNA polymerase (New England Biolabs) or 5 U AmpliTaq DNA polymerase (Perkin Elmer). The reaction mixture was denatured at 94°C for 5 min and 30–35 cycles—denaturation at 94°C for 30 s, annealing at 42–50°C for 30 s, and extension at 72°C for 1.5–3 min—were performed using a MJ Research Mini-Cycler (Watertown, MA). The reaction products were analyzed by agarose gel electrophoresis. Each PCR reaction was repeated in an independent experiment.

Chromosome mapping. The genetic map position of the IGRP gene was determined using the Jackson Laboratory Backcross DNA Mapping Resource panels (40) and was given the designation *G6pc-rs*. DNA from 94 interspecific BSS backcross progeny [(C57BL/6JEi × SPRET/Ei)F1 × SPRET/Ei] and DNA from 94 progeny from the reciprocal BSB cross [(C57BL/6JEi × SPRET/Ei)F1 × C57BL/6JEi] were analyzed by PCR. The PCR primers used represent the IGRP gene sense strand sequence between –865 and –840 (5′-CTGAAAGTTGTC CTCTGACCTCTACA-3′) and antisense strand sequence between –695 and –720 (5′-GTAGAAGTATGTTTGAACTGAACTAT-3′). These primers were designed to encompass a IGRP promoter region that contained multiple repeats of the sequences TACA, CAT, CAG, and CAA and thus was likely to be polymorphic (Fig. 4*A*). Each PCR reaction contained 5 ng of genomic DNA, 2.0 mmol/l $MgCl_2$, 1 µmol/l of each primer, 200 µmol/l of each dNTP, 1× supplied reaction buffer, and 0.5 U Taq DNA polymerase (Perkin Elmer) in a 25-µl reaction. Cycling conditions consisted of an initial denaturation step for 4 min at 94°C followed by 35 cycles—94°C for 30 s, 55°C for 30 s, 72°C for 30 s—with a final extension incubation at 72°C for 10 min. The IGRP gene–specific primers amplified products of 180 and 200 bp with B6 and SPRET, respectively. Amplified products were run on 4% agarose gels and visualized after ethidium bromide staining with ultraviolet light.

RNA isolation and primer extension analysis. βTC-3 total RNA was isolated using a modification of previous methods (41,42). Briefly, βTC-3 cells (four 55-cm^2 dishes) were lysed and homogenized in 7 ml of a solution containing 50 mmol/l Tris (pH 7.5), 5 mol/l guanidine thiocyanate, 0.5% (vol/vol) β-mercaptoethanol, and 17 mmol/l sodium lauryl sarcosinate. Two and one-half milliliters of 6 mol/l CsCl, 0.1 mol/l EDTA was added and mixed by homogenization, and the suspension was layered over a 2-ml cushion of 6 mol/l CsCl, 0.1 mol/l EDTA in a SW41 polyallomer tube (Beckman, Palo Alto, CA). The RNA was pelleted by centrifugation at 24,000 rpm for 20 h at 20°C. The yield of RNA was ~50 µg per 55 cm^2 dish. A 26-bp primer (5′-GCACTCCACTCCTATGAAGGAAATCC-3′), complementary to exon 1, was synthesized by the Vanderbilt University Medical School Diabetes Core laboratory and, following gel purification (43), was then 5′ end-labeled with [γ-^{32}P]ATP to a specific activity of ~2 Ci/µmol (43). The labeled primer (~3 × 10^5 cpm) was annealed to 10 µg of total βTC-3 RNA for 1 h at 60°C, and primer extension was performed as previously described (44).

Fusion gene plasmid construction. The construction of a mouse G-6-Pase catalytic subunit-chloramphenicol acetyltransferase (CAT) fusion gene, containing promoter sequence from –751 to +66, in the pCAT(An) expression vector (45), has been previously described (14). An IGRP-CAT fusion gene was constructed in the pCAT(An) expression vector as follows: the IGRP gene promoter was isolated from the pGEM-Bac 4 · 8 plasmid (Fig. 1) as a *Hin*dIII-*Pst*I fragment and subcloned into *Hin*dIII-*Pst*I–digested pSP72 (Promega, Madison, WI). The promoter fragment was then isolated from the pSP72 plasmid as a *Hin*dIII-*Bam*HI fragment and ligated into *Hin*dIII-*Bgl*II–digested pCAT(An). The resulting plasmid contains IGRP promoter sequence from –911 to +3, relative to the transcription start site. The pCAT(An) vector has polyadenylation signals located 5′ of the polylinker to prevent read-through transcription (45). Control experiments demonstrated that there was no increase in background CAT activity when the empty vector, minus the G-6-Pase catalytic subunit or IGRP gene promoters, was transiently transfected into HIT or HepG2 cells (data not shown).

A series of truncated IGRP-CAT fusion genes was generated by restriction enzyme digestion of the –911 IGRP-CAT construct with one of the following enzymes: *Bgl*II, *Nhe*I, *Afl*II, *Xmn*I, or *Afl*III. The resulting plasmids have calculated 5′ end points of –508, –306, –273, –197, and –66, which were confirmed by DNA sequencing using the USB Sequenase kit. All plasmid constructs were purified by centrifugation twice through cesium chloride gradients (43).

Cell culture and transient transfection. Two cell lines were used. Human HepG2 hepatoma cells were grown to 40–70% confluence in Dulbecco's modified Eagle's medium (DMEM) containing 2.5% (vol/vol) newborn calf serum, 2.5% (vol/vol) fetal calf serum, and 5% (vol/vol) Nu serum IV (Becton Dickinson, Bedford, MA). Cells from individual T150 flasks were harvested by trypsinization, pelleted by centrifugation, and resuspended in 2 ml of a calcium phosphate–DNA coprecipitate containing 60 µg reporter plasmid DNA and 10 µg of an expression vector encoding β-galactosidase (14,46,47). The cells were immediately replated into four 55-cm^2 culture dishes (0.5 ml/dish) containing 10 ml DMEM supplemented with 2.5% (vol/vol) newborn calf serum and 2.5% (vol/vol) fetal calf serum. The cells were then returned to a humidified 5% CO_2, 95% air atmosphere in a Nuaire (Plymouth, MN) cell culture incubator. Six hours after transfection, the cells were treated for 5 min with 20% (vol/vol) DMSO in serum-containing DMEM (5 ml/dish), washed for 5 min in serum-containing and then serum-free DMEM (each 5 ml/dish), and then incubated for 18–20 h in serum-free DMEM (10 ml/dish).

HIT cells were grown to 70% confluence in T150 flasks in DMEM containing 2.5% (vol/vol) fetal bovine serum and 15% (vol/vol) horse serum and were replated the day before use into 55-cm^2 culture dishes (1 flask to 12 dishes). Attached cells were then transfected by addition of 0.5 ml of a calcium phosphate–DNA coprecipitate containing 15 µg reporter plasmid DNA and 2.5 µg of an expression vector encoding β-galactosidase (14,47) to the 10 ml of culture medium. The cells were then returned to a humidified 5% CO_2, 95% air atmosphere in a Nuaire cell culture incubator. After incubation for between 4 and 6 h, the cells were treated for 2 min with 20% glycerol in serum-free DMEM (5 ml/dish). The cells were then rinsed for 5 min with serum-free DMEM (5 ml/dish) before incubation for 18–20 h in serum-free DMEM (10 ml/dish).

CAT and β-galactosidase assays. Cells were harvested by trypsin digestion and sonicated in 300 µl of 250 mmol/l Tris (pH 7.8) containing 2 mmol/l phenylmethylsulfonyl fluoride (PMSF). After sonication, a sample of the supernatant was assayed for β-galactosidase activity as described (48). The remaining supernatant was heated for 10 min at 65°C, and cellular debris was removed by centrifugation. CAT assays were then performed on the supernatant as described previously (47). To correct for variations in transfection efficiency, the results are expressed as a ratio of CAT:β-galactosidase activity, and two to three independent preparations of each plasmid construct were analyzed.

RESULTS AND DISCUSSION

Isolation of the IGRP gene. To isolate the IGRP gene, a mouse BAC library was probed with a mouse IGRP cDNA, designated 1B1 (34), that contained the entire open reading frame. Three positive clones were identified, one of which gave a much stronger hybridization signal than the others. This clone, designated BAC IGRP-3, was selected for further analysis on the assumption that it contained a greater proportion of the IGRP gene; it was subsequently found to contain the entire IGRP transcription unit (Fig. 1).

BAC IGRP-3 DNA was digested with a panel of restriction enzymes and probed by hybridization with labeled fragments representing either the 5′ or 3′ ends of the IGRP cDNA. Two *Xba*I-*Xba*I fragments were identified, ~4.8 and ~4.5 kbp in size, that specifically hybridized to the 5′ and 3′ IGRP cDNA probes, respectively. These fragments were gel-purified and ligated into the pGEM7 plasmid vector for further analysis. The resulting plasmids, designated pGEM-BAC 4.8 and pGEM-BAC 4.5, were both subsequently found to represent partial *Xba*I digestion products (Fig. 1).

Exon/intron structure of the IGRP gene. The exon/intron structure of the IGRP gene (Fig. 1 and Table 1) was determined by either direct DNA sequencing of the IGRP-pGEM7 plasmid subclones or, for introns A–C, by PCR using BAC IGRP-3 DNA as the template. Exon/intron splice junctions were identified by comparing the IGRP genomic and cDNA sequences. The predicted exon/intron splice sites (Table 2) were then determined by comparison with the splice consensus sequence (49) and, where the sequence differed from the consensus, by the requirement that the IGRP open reading frame be maintained.

The mouse IGRP gene, like the genes encoding the human, mouse, and rat G-6-Pase catalytic subunit (6,7,23), is composed of five exons (Table 1). The sizes of exons 2 and 4 are identical between the two genes, whereas exon 3 is 6 bp larger in the IGRP gene (Table 1), which corresponds to the insertion of two amino acids, as seen in the alignment of peptide sequences (34). The sizes of the four introns are also similar between the mouse IGRP (Fig. 1) and mouse G-6-Pase catalytic subunit genes (7), with the exception of intron A, which is considerably smaller in the IGRP gene. The latter accounts for the fact that the IGRP gene only spans ~8 kbp (Fig. 1), whereas the mouse G-6-Pase catalytic subunit gene spans ~10 kbp (7).

An alignment of the exon/intron boundaries comparing the mouse IGRP gene and the rat and mouse G-6-Pase catalytic subunit genes (7,23) shows that these junctions are also well conserved, with the exception of the boundary between intron C and the 5′ end of exon 4 (Table 2). Apart from this

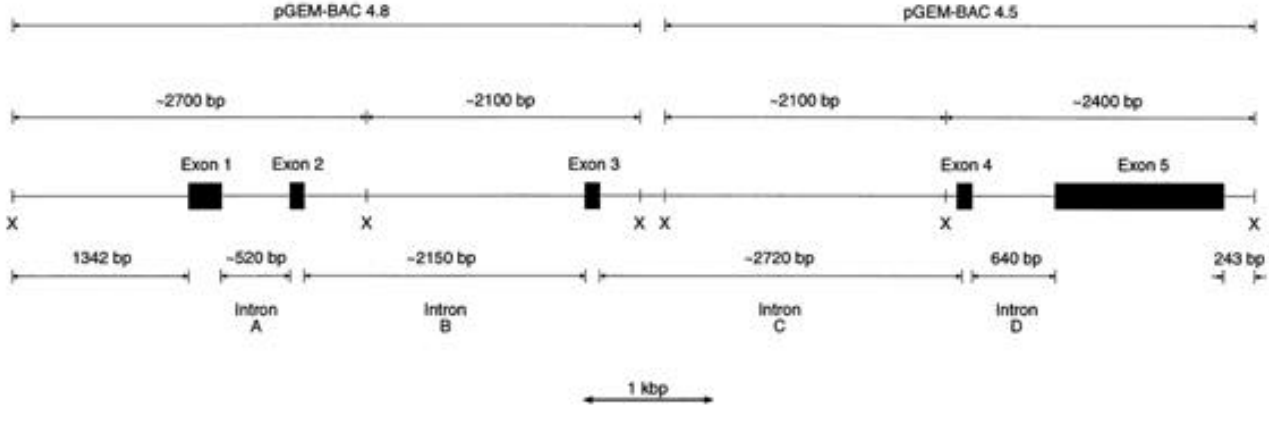

FIG. 1. Structure of the mouse IGRP gene. The IGRP gene exon and intron sizes were determined by a combination of direct DNA sequencing and PCR as described in METHODS. X, *Xba*I.

TABLE 1
Comparison of exon sizes between the IGRP and G-6-Pase catalytic subunit genes

Exon number	Exon size (bp)	
	G-6-Pase	IGRP
1	311	254
2	110	110
3	106	112
4	116	116
5	1,615	1,284

The mouse G-6-Pase catalytic subunit gene exon sizes are from Shelly et al. (7); the IGRP gene exon sizes were determined as described in METHODS.

one exception, the sequence of the 5′ and 3′ exon/intron junctions corresponds well with the consensus splice sequences (49). We hypothesize that the change in the nucleotide at the 5′ end of exon 4 from the consensus G to an A may explain the frequent removal of exon 4 by differential splicing as reported by Arden et al. (34) (Table 2). Haber et al. (50) have reported a similar observation in the rat G-6-Pase catalytic subunit gene. In rat liver, it appears that 20% of G-6-Pase catalytic subunit transcripts represent a splicing variant in which exon 2 is deleted despite the presence of a consensus splice sequence (Table 2) (50). It remains to be determined whether this splicing is a regulated event but, at least following partial hepatectomy, there is no consistent variation in the relative ratios of full-length and exon 2–deleted G-6-Pase catalytic subunit RNA transcripts (50). Similarly, in various diabetic animal models, there is no consistent variation in the relative ratios of full-length and exon 4–deleted IGRP RNA transcripts (34). Furthermore, the spliced variants of both the IGRP (34) and G-6-Pase catalytic subunit (50) RNA transcripts are predicted to encode truncated, presumably nonfunctional, proteins.

The sequence of the five IGRP exons as determined from genomic DNA was identical to that reported for the IGRP cDNA (34), with the exception of three base pairs, all of which are found in the 3′ untranslated region. Thus nucleotide 1755 is a G in the genomic sequence and a C in the cDNA sequence; nucleotide 1647 is an A in the genomic sequence and a G in the cDNA sequence; and an additional A is inserted in genomic sequence within a string of nine A's starting at nucleotide 1697. These nucleotides are numbered relative to the experimentally determined major transcription start site, which is located at +27 relative to the longest IGRP cDNA isolated (34).

Chromosomal mapping of the IGRP gene. Two interspecific backcross DNA mapping panels were used to unambiguously localize the IGRP gene to the proximal portion of chromosome 2 (Fig. 2). The chromosome 2 map position of the IGRP gene has been given the designation *G6pc-rs* (Fig. 2). The simple sequence repeat marker *D2Mit11*, positioned at 39 cM, had been scored previously in both backcross panels. No recombinants between this marker and *G6pc-rs* were found in either backcross panel (0 of 188) (Fig. 2). The acetylcholine receptor alpha (*Acra*), also mapped in both backcross panels, was sited 1.6 ± 0.9 cM distal to *G6pc-rs* (Fig. 2).

The expected position of an orthologous gene for mouse *G6pc-rs* in humans would be on chromosome 2q. The chromosomal location of the gene encoding the mouse G-6-Pase catalytic subunit is unknown, although the human gene maps to chromosome 17 (51). Based on the close homology between the human and mouse genomes, however, the mouse ortholog for the G-6-Pase catalytic subunit would be expected to be on chromosome 11. Thus, the position of the mouse IGRP gene does not map to a G-6-Pase catalytic subunit encoding locus, which is consistent with a level of ~50% homology between the nucleotide sequences of the mouse IGRP cDNA (34) and the mouse G-6-Pase catalytic subunit cDNA (7).

We have considered the possibility that the IGRP gene might encode a component of the G-6-Pase complex other

TABLE 2
Comparison of the exon/intron boundaries between the mouse IGRP and mouse and rat G-6-Pase catalytic subunit genes

Intron	Gene	5′ Intron junction	3′ Intron junction
A	Mouse IGRP	TTTAAATG/gtaaga	cag/GATATTGTTTGG
	Rat G-6-Pase	TTTAAGTG/gtaaga	cag/GATTCTTTTTGG
	Mouse G-6-Pase	TTCAAGTG/	/GATTCTGTTTGG
B	Mouse IGRP	ACAGGCCCAG/gtaagca	tgctcattgcag/GAAGTCCATCTG
	Rat G-6-Pase	ACTGGACCAG/gt**g**agca	tgc-catt**t**-ag/GGAGTCCCTCGG
	Mouse G-6-Pase	ACCGGACCAG/	/GAAGTCCCTCTG
C	Mouse IGRP	TCTGCACAG/gtcag	ttccatcacag/ACTGACCTGGTC
	Rat G-6-Pase	TGGATTCCG/gt**a**ag	tt**gtc**tt**g**cag/GTGCTTGAATGT
	Mouse G-6-Pase	TGGATTCCG/	/GTGTTTGAACGT
D	Mouse IGRP	TGGAGTGATTGGTG/gtaaatatagc	tccaatccccag/GGATGCTAGTAG
	Rat G-6-Pase	TGGAGTCTTGTCAG/gta**tcagca**gc	tc**tgcca**ca**c**ag/GCATTGCTGTGG
	Mouse G-6-Pase	TGGAGTCTTGTCAG/	/GCATTGCTGTGG
	Consensus sequence	(A or T) G/gtaa	cag/G 3′

The mouse and rat G-6-Pase catalytic subunit gene exon/intron boundaries are from Shelly et al. (7) and Argaud et al. (23), respectively, whereas the IGRP gene exon/intron boundaries were determined as described in METHODS. The intron sequences of the mouse G-6-Pase catalytic subunit gene have not been published. Exon and intron sequences are shown in uppercase and lowercase letters, respectively. Regions of sequence divergence between the mouse IGRP gene and the mouse and rat G-6-Pase catalytic subunit genes are underlined (exon sequence) or are in bold type (intron sequence). The 5′ and 3′ consensus splice sequences are from Jackson (49).

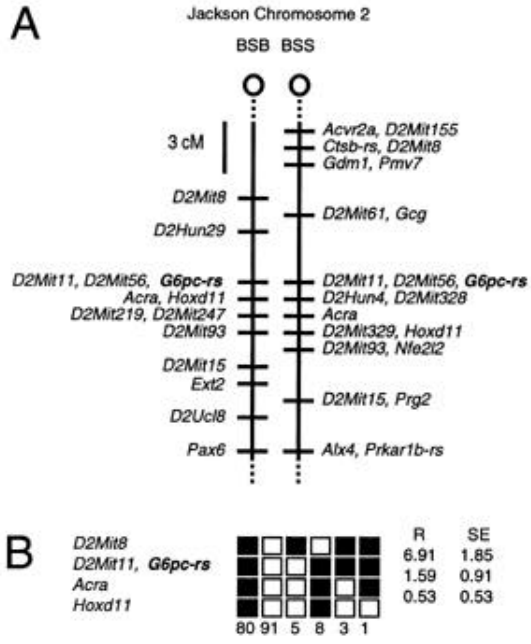

FIG. 2. Chromosomal location of the IGRP gene. A map (*A*) and haplotype (*B*) diagram are shown in which the IGRP gene (map location designated as *G6pc-rs*) is localized to the proximal arm of chromosome 2 in the Jackson Laboratory BSB and BSS backcross DNA panels. *A*: The map with the centromere toward the top. A 3-cM scale bar is shown to the right of the figure. Loci mapping to the same position are listed in alphabetical order. *B*: Haplotype figure from the Jackson Laboratory BSS backcross showing part of chromosome 2 with loci linked to *G6pc-rs*. Loci are listed in order with the most proximal at the top. The black boxes indicate the C57BL/6JEi allele and the white boxes the SPRET/Ei allele. The number of backcross progeny for each genotype is indicated at the bottom of each haplotype. Recombination frequencies ± SE between markers at the 95% confidence level are shown for the 188 mice from both mapping panels. Complete typing data for the BSB and BSS panel are available at the following URL: http://www.jax.org/resources/documents/cm_data.

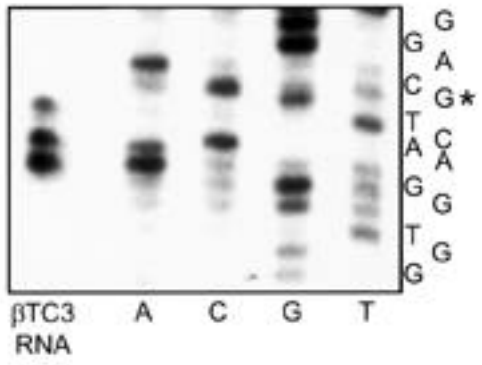

FIG. 3. Determination of the mouse IGRP gene transcription start site. To locate the mouse IGRP gene transcription initiation site, a primer extension assay was performed, as described in METHODS, using mouse βTC-3 RNA and an oligonucleotide primer complementary to exon 1. A dideoxynucleotide sequencing reaction (labeled A,C,G,T) was also performed using the pGEM-BAC 4.8 plasmid (see Fig. 1) as the template and the same exon 1 primer. The products of the dideoxynucleotide sequencing reaction and primer extension reaction were separated on the same denaturing polyacrylamide gel, which allowed for a direct comparison of the major extended products with their corresponding initiation bases. The position of the most 5′ major primer extension product is indicated (*).

than the catalytic subunit. Glycogen storage disease (GSD) type 1a is due to mutations in the gene encoding the G-6-Pase catalytic subunit, whereas GSD types 1b and 1c are thought to be due to mutations in genes encoding two of the other components of the G-6-Pase complex, namely the glucose-6-phosphate and the phosphate/pyrophosphate transporters, respectively (3–5,51–53). Interestingly, the genes responsible for GSD type 1b (52) and type 1c (53) have recently both been broadly mapped to the 11q23 region on human chromosome 11. Thus this location is not consistent with the expected position of an orthologous gene for mouse *G6pc-rs* in humans, which is on chromosome 2q.

Determination of the IGRP gene transcription start site. To determine the transcription start site of the IGRP gene, a primer extension analysis was performed using RNA isolated from βTC-3 cells (Fig. 3). Several transcription start sites were detected, the most prominent of which were clustered over a 5-bp region (Fig. 3). The most 5′ of these major transcription start sites was designated +1. A consensus TATA box sequence (TATA) is present in the promoter 25 bp upstream from this position (Fig. 4*B*). Overexposure of the autoradiograph revealed several weak upstream transcription start sites, the most 5′ of which was at position –26, which corresponds to the 5′ end of the longest IGRP cDNA isolated (34). A nonconsensus TATA box sequence (TAAT) is present in the promoter 28 bp upstream from this base (Fig. 4*B*).

Tissue-specific activity of the IGRP gene promoter. An alignment of the putative IGRP promoter sequence (Fig. 4*A*) with that of the mouse G-6-Pase catalytic subunit promoter revealed a stretch of ~50% homology, not including spaces, over the –252 to 1 region (Fig. 4*B*). None of the *cis*-acting elements identified in the mouse G-6-Pase catalytic subunit promoter, including an hepatocyte nuclear factor (HNF)-1 binding site (15), three insulin response sequence (IRS) motifs (14), or the TATA box are conserved (Fig. 4*B*). By contrast, all of these *cis*-acting elements are highly conserved between the mouse, rat, and human G-6-Pase catalytic subunit promoters (13–15,23,54).

To investigate the activity of the putative IGRP promoter region, an IGRP-CAT fusion gene was constructed, containing IGRP promoter sequence between –911 and +3, in the expression vector pCAT(An) (45). This IGRP-CAT fusion gene was transiently transfected into the HIT and HepG2 cell lines, which are representative of pancreatic islet β-cells and liver cells, respectively, and basal IGRP-CAT expression was compared with that obtained with a mouse G-6-Pase catalytic subunit-CAT fusion gene containing promoter sequence from –751 to +66 (Fig. 5). The relative basal expression of these fusion genes varied dramatically between the two cell lines (Fig. 5). Thus, in HIT cells, basal IGRP-CAT expression was ~150-fold higher than basal G-6-Pase-CAT expression. In contrast, in HepG2 cells the IGRP promoter is inactive, whereas high basal G-6-Pase-CAT expression is detected (Fig. 5). This complete lack of IGRP promoter activity in HepG2 cells was somewhat surprising given the relatively high sequence homology over the proximal regions of the G-6-Pase and IGRP promoters (Fig. 4*B*). To investigate the possibility that the proximal IGRP promoter might be active in HepG2 cells in the absence of distal promoter sequences, we constructed a series of truncated IGRP-CAT fusion genes. None of these constructs conferred an increase in CAT activity over the assay background when transiently transfected into HepG2 cells (data not shown). It is apparent, however,

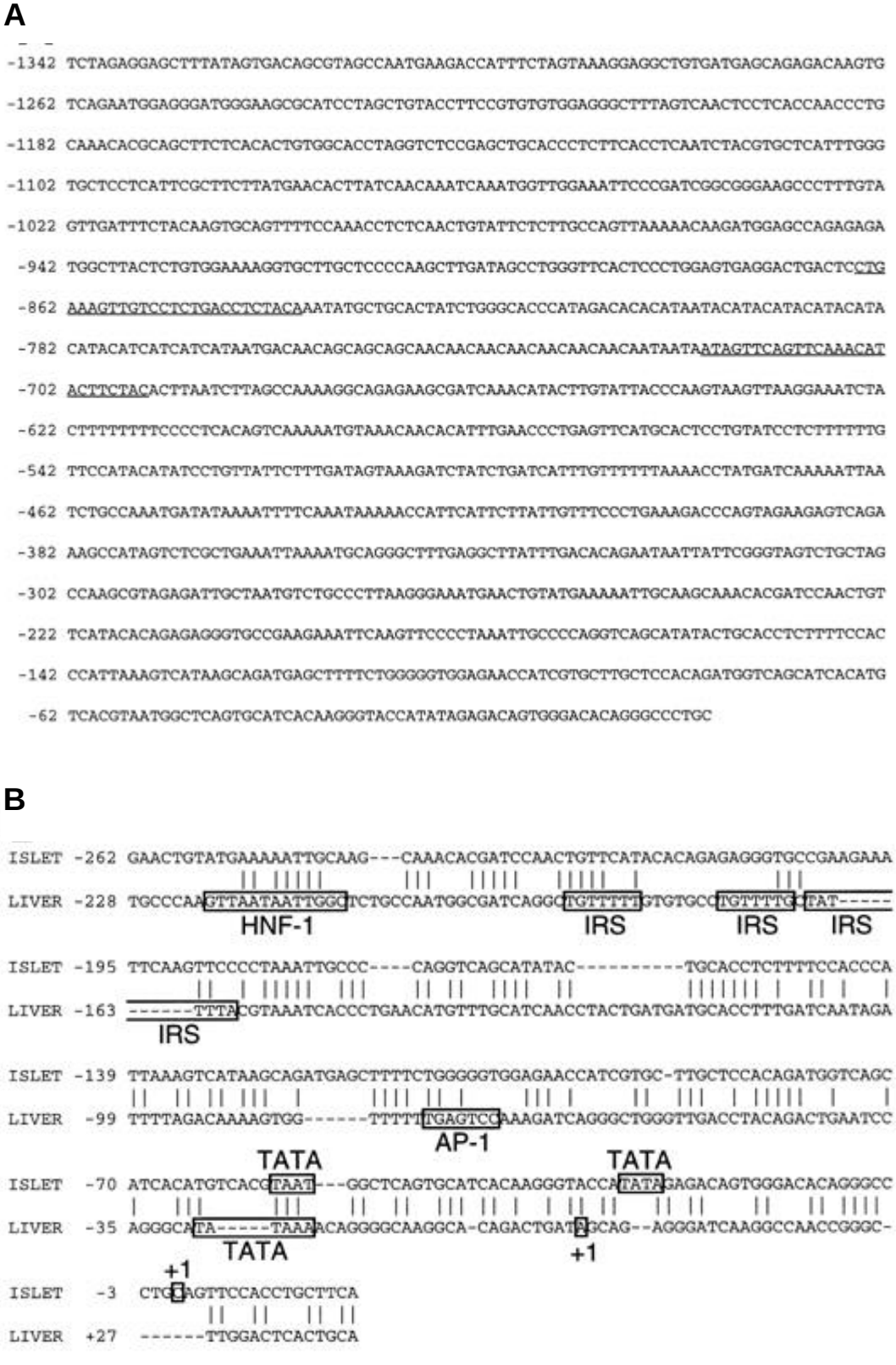

FIG. 4. IGRP gene promoter sequence and alignment with that of the G-6-Pase catalytic subunit gene promoter. *A*: Sequence of the mouse IGRP promoter between –1342 and +1. The location of the primers used to map the chromosomal location of the IGRP gene, located either side of a polymorphic region of the promoter, are underlined. *B*: The mouse IGRP and mouse G-6-Pase catalytic subunit promoter sequences were aligned using the IntelliGenetics IFIND program. The *cis*-acting elements identified in the mouse G-6-Pase catalytic subunit promoter, including the TATA box, a HNF-1 binding site (15,54), three IRS motifs (14), and a putative activator protein-1 (AP-1) binding site, are boxed, as are two putative TATA boxes in the IGRP promoter. The transcription start sites of the two genes are designated as +1.

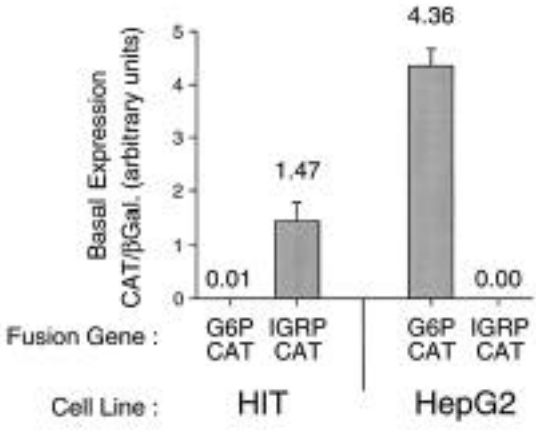

FIG. 5. Comparison of the relative basal activities of the IGRP and G-6-Pase catalytic subunit gene promoters. HIT cells and HepG2 cells were transiently cotransfected, as described in METHODS, with an expression vector encoding β-galactosidase (2.5 μg) and either an IGRP-CAT or G-6-Pase-CAT fusion gene (15 μg) containing promoter sequences from –911 to +3 and –751 to +66, respectively. After transfection, cells were incubated for 18–20 h in serum-free medium. The cells were then harvested, and both CAT and β-galactosidase activities were assayed as previously described (14,47). Results are presented as the ratio of CAT to β-galactosidase activity and represent the means ± SE of three experiments, each using an independent preparation of both plasmids.

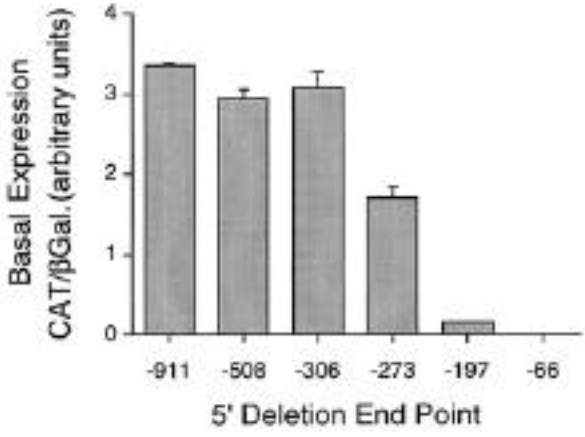

FIG. 6. The proximal IGRP promoter sequence between –306 and +3 is sufficient to confer high basal reporter gene expression in HIT cells. HIT cells were transiently cotransfected, as described in METHODS, with a series of IGRP-CAT fusion genes (15 μg), with 5′ deletion end points as shown on the abscissa, and with an expression vector encoding β-galactosidase (2.5 μg). After transfection, cells were incubated for 18–20 h in serum-free medium. The cells were then harvested, and both CAT and β-galactosidase activities were assayed as previously described (14,47). Results are presented as the ratio of CAT to β-galactosidase activity and represent the means ± SE of three to four experiments.

that the proximal IGRP promoter region located between –306 and +3 is sufficient to confer maximal basal IGRP-CAT fusion gene expression in HIT cells (Fig. 6). Interestingly, Shelton et al. (55) have previously shown that the proximal region of the upstream glucokinase promoter, located between –280 and +14, is also sufficient to confer maximal basal expression of that gene in HIT cells.

Experiments are currently in progress to identify the *cis*-acting elements that are required for the islet cell–specific expression of the IGRP gene. From the initial analysis of a limited series of IGRP-CAT fusion genes transiently transfected into HIT cells, it is already apparent that multiple *cis*-acting elements in the –306 to +3 promoter region are required for high basal reporter gene expression (Fig. 6). To date, only a few other islet cell–specific genes have been identified, such as those encoding insulin (56), glucagon (57), and islet amyloid polypeptide (amylin) (58). The promoters of these genes have been analyzed in varying degrees of detail (56–58). The results suggest that islet-specific transcription factors do not exist; rather, islet-specific expression is conferred by the particular arrangement of transcription factors binding the promoter (56).

Multiple hormones and signaling molecules regulate the hepatic expression of the G-6-Pase catalytic subunit gene. Thus, glucocorticoids, cAMP, glucose, and fatty acids all increase G-6-Pase catalytic subunit mRNA levels (23,25,59–63), whereas insulin, tumor necrosis factor-α, and interleukin-6 all repress basal G-6-Pase catalytic subunit gene expression (13,14,23,59,64,65). Insulin treatment also overrides the stimulatory effects of cAMP, glucocorticoids, glucose, and fatty acids on G-6-Pase catalytic subunit gene expression (13,14,23,25,59,60,63). With the exception of insulin (14,15) and cAMP (54), little is known of the *cis*-acting elements that mediate the actions of these factors on G-6-Pase catalytic subunit gene expression; whether any of these factors also regulate expression of the IGRP gene remains to be determined.

Tokuyama et al. (35) have shown, using RT-PCR in conjunction with primers that would not be expected to anneal to the IGRP cDNA sequence, that the gene encoding the catalytic subunit of G-6-Pase is expressed in islets. It remains to be determined, however, whether the same promoter that drives expression of the G-6-Pase catalytic subunit in liver is also active in islets. Although the use of alternative, tissue-specific promoters is relatively rare, Magnuson and colleagues (66) have clearly demonstrated that alternative promoters drive the expression of the gene encoding glucokinase (hexokinase IV) in liver and islets. It is apparent, though, that while the activity of the mouse G-6-Pase catalytic subunit promoter was low in HIT cells relative to the IGRP promoter, basal G-6-Pase-CAT fusion gene expression was detected (Fig. 5).

The IGRP lacks detectable G-6-Pase activity (34), but whether this is indicative of a missing component in the G-6-Pase assay or is simply because the IGRP catalyzes a distinct biochemical reaction remains to be determined. However, the alternative possibility exists that the IGRP is a nonfunctional gene product and represents a vestigial evolutionary event. This seems unlikely given the abundance of IGRP mRNA in islets and the conservation of critical catalytic residues between the IGRP and G-6-Pase catalytic subunit (34), but some indirect insight into this possibility will be obtained by cloning the human IGRP cDNA and gene. Furthermore, a comparison of the mouse and human IGRP promoter sequences would facilitate the identification of important conserved *cis*-acting elements, as previously exemplified by studies on the phosphoenolpyruvate carboxykinase gene promoter, for example (48). It should be noted, however, that recent studies in transgenic mice have led to an increased awareness of the fact that mouse and human islets are not identical. Thus, homozygous deletion of the gene encoding HNF-1α in mice results in defective insulin secretion (67), as well as other abnormalities (68,69), while heterozygous HNF-1α (+/–) mice are normal (67–69). By contrast,

deletion of the HNF-1α gene in humans is thought to be lethal, whereas individuals who are heterozygous for HNF-1α mutations have severe insulin secretory defects (30,70). The concept that rodent and human islets are different is more directly supported by the observation that the abundance of the GLUT2 glucose transporter is 100-fold lower in human versus rat islet β-cells (71).

In summary, this paper describes the cloning of the IGRP gene and initial characterization of the IGRP promoter. Future studies will focus on the identification of the *cis*-acting elements that confer the islet-specific expression of the IGRP gene, as well as addressing the question whether IGRP expression is regulated in response to hormones or nutrients.

ACKNOWLEDGMENTS

Data analysis was performed in part through the use of the Vanderbilt University Medical Center Cell Imaging Resource (CA68485 and DK20593), and the research was supported by grants from the NIH (RR 08911, DK36175, DK27722 to E.H.L. and GM07347 to D.H.E.), the Juvenile Diabetes Foundation (E.H.L. and R.M.O.), the Vanderbilt University Research Council, the Mark Collie Foundation, and the American Diabetes Association (to R.M.O.). C.E.M. is a fellow of the American Diabetes Association.

We thank Mark Magnuson for providing the mouse BAC library, Howard Towle for the pCAT(An) expression vector plasmid, Richard Printz for both useful advice on the cloning strategy and comments on the manuscript, Roland Stein and Eva Henderson for providing the HIT cell line, and Shimon Efrat for providing the βTC-3 cell line. We also thank Lucy Rowe and Mary Barter for kindly providing the resources of the Jackson Laboratory Backcross DNA Panel Map Service and Rebecca Taub for useful discussions on the potential role of G-6-Pase in islets.

Note Added in Proof: The DNA sequences described in this manuscript have been submitted to GenBank and have been given the Accession Numbers AF118761–AF118766.

REFERENCES

1. Flakoll P, Carlson MG, Cherrington A: Physiologic action of insulin. In *Diabetes Mellitus. A Fundamental and Clinical Text*. LeRoith D, Taylor SI, Olefsky JM, Eds. Philadelphia, PA, Lippincott-Raven, 1996, p. 121–132
2. Cersosimo E, Molina PE, Abumrad NN: Renal lactate metabolism and gluconeogenesis during insulin-induced hypoglycemia. *Diabetes* 47:1101–1106, 1998
3. Burchell A: Molecular pathology of glucose-6-phosphatase. *FASEB J* 4:2978–2988, 1990
4. Mithieux G: New knowledge regarding glucose-6 phosphatase gene and protein and their roles in the regulation of glucose metabolism. *Eur J Endocrinol* 136:137–145, 1997
5. Foster JD, Pederson BA, Nordlie RC: Glucose-6-phosphatase structure, regulation, and function: an update. *Proc Soc Exp Biol Med* 215:314–332, 1997
6. Lei K-J, Shelly LL, Pan C-J, Sidbury JB, Chou JY: Mutations in the glucose-6-phosphatase gene that cause glycogen storage disease type 1a. *Science* 262:580–583, 1993
7. Shelly LL, Lei K-J, Pan C-J, Sakata SF, Ruppert S, Schutz G, Chou JY: Isolation of the gene for murine glucose-6-phosphatase, the enzyme deficient in glycogen storage disease type 1a. *J Biol Chem* 268:21482–21485, 1993
8. Gerin I, Veiga-da-Cunha M, Achouri Y, Collet JF, Van Schaftingen E: Sequence of a putative glucose 6-phosphate translocase, mutated in glycogen storage disease type 1b. *FEBS Lett* 419:235–238, 1997
9. Waddell ID, Zomerschoe AG, Voice MW, Burchell A: Cloning and expression of a hepatic microsomal glucose transport protein. *Biochem J* 286:173–177, 1992
10. DeFronzo RA, Bonadonna RC, Ferrannini E: Pathogenesis of NIDDM. *Diabetes Care* 15:318–368, 1992
11. Consoli A: Role of liver in pathophysiology of NIDDM. *Diabetes Care* 15:430–441, 1992
12. Cline GW, Rothman DL, Magnusson I, Katz LD, Shulman GI: ^{13}C-nuclear magnetic resonance spectroscopy studies of hepatic glucose metabolism in normal subjects and subjects with insulin-dependent diabetes mellitus. *J Clin Invest* 94:2369–2376, 1994
13. Schmoll D, Allan BB, Burchell A: Cloning and sequencing of the 5′ region of the human glucose-6-phosphatase gene: transcriptional regulation by cAMP, insulin and glucocorticoids in H4IIE hepatoma cells. *FEBS Lett* 383:63–66, 1996
14. Streeper RS, Svitek CA, Chapman S, Greenbaum LE, Taub R, O'Brien R.M: A multi-component insulin response sequence mediates a strong repression of mouse glucose-6-phosphatase gene transcription by insulin. *J Biol Chem* 272:11698–11701, 1997
15. Streeper RS, Eaton EM, Ebert DH, Chapman S, Svitek CA, O'Brien RM: Hepatocyte nuclear factor-1 acts as an accessory factor to enhance the inhibitory action of insulin on mouse glucose-6-phosphatase gene transcription. *Proc Natl Acad Sci U S A* 95:9208–9213, 1998
16. Efendic S, Karlander S, Vranic M: Mild type II diabetes markedly increases glucose cycling in the postabsorptive state and during glucose infusion irrespective of obesity. *J Clin Invest* 81:1953–1961, 1988
17. Granner DK, O'Brien RM: Molecular physiology and genetics of NIDDM. Importance of metabolic staging. *Diabetes Care* 15:369–395, 1992
18. Barzilai N, Rossetti L: Role of glucokinase and glucose-6-phosphatase in the acute and chronic regulation of hepatic glucose fluxes by insulin. *J Biol Chem* 268:25019–25025, 1993
19. Seoane J, Trinh K, O'Doherty RM, Gomez-Foix AM, Lange AJ, Newgard CB, Guinovart JJ: Metabolic impact of adenovirus-mediated overexpression of the glucose-6-phosphatase catalytic subunit in hepatocytes. *J Biol Chem* 272:26972–26977, 1997
20. Burchell A, Cain DI: Rat hepatic microsomal glucose-6-phosphatase protein levels are increased in streptozotocin-induced diabetes. *Diabetologia* 28:852–856, 1995
21. Liu Z, Barrett EJ, Dalkin AC, Zwart AD, Chou JY: Effect of acute diabetes on rat hepatic glucose-6-phosphatase activity and its messenger RNA level. *Biochem Biophys Res Commun* 205:680–686, 1994
22. Haber BA, Chin S, Chuang E, Buikhuisen W, Naji A, Taub R: High levels of glucose-6-phosphatase gene and protein expression reflect an adaptive response in proliferating liver and diabetes. *J Clin Invest* 95:832–841, 1995
23. Argaud D, Zhang Q, Pan W, Maitra S, Pilkis SJ, Lange AJ: Regulation of rat liver glucose-6-phosphatase gene expression in different nutritional and hormonal states. *Diabetes* 45:1563–1571, 1996
24. Mithieux G, Vidal H, Zitoun C, Bruni N, Daniele N, Minassian C: Glucose-6-phosphatase mRNA and activity are increased to the same extent in kidney and liver of diabetic rats. *Diabetes* 45:891–896, 1996
25. Massillon D, Barzilai N, Chen W, Hu M, Rossetti L: Glucose regulates *in vivo* glucose-6-phosphatase gene expression in the liver of diabetic rats. *J Biol Chem* 271:9871–9874, 1996
26. Polonsky KS: The beta-cell in diabetes: from molecular genetics to clinical research. *Diabetes* 44:705–717, 1995
27. Poitout V, Robertson RP: An integrated view of beta-cell dysfunction in type-II diabetes. *Ann Rev Med* 47:69–83, 1996
28. Yamagata K, Furuta H, Oda N, Kaisaki PJ, Menzel S, Cox NJ, Fajans SS, Signorini S, Stoffel M, Bell GI: Mutations in the hepatocyte nuclear factor-4alpha gene in maturity-onset diabetes of the young (MODY1). *Nature* 384:458–460, 1996
29. Vionnet N, Stoffel M, Takeda J, Yasuda K, Bell GI, Zouali H, Lesage S, Velho G, Iris F, Passa P, Froguel P, Cohen D: Nonsense mutation in the glucokinase gene causes early-onset non-insulin-dependent diabetes mellitus. *Nature* 356:721–722, 1992
30. Yamagata K, Oda N, Kaisaki PJ, Menzel S, Furuta H, Vaxillaire M, Southam L, Cox RD, Lathrop GM, Boriraj VV, Chen X, Cox NJ, Oda Y, Yano H, Le Beau MM, Yamada S, Nishigori H, Takeda J, Fajans SS, Hattersley AT, Iwasaki N, Hansen T, Pedersen O, Polonsky KS, Turner RC, Velho G, Chevre J-C, Froguel P, Bell GI: Mutations in the hepatocyte nuclear factor-1alpha gene in maturity-onset diabetes of the young (MODY3). *Nature* 384:455–458, 1996
31. Stoffers DA, Ferrer J, Clarke WL, Habener JF: Early-onset type-II diabetes mellitus (MODY4) linked to IPF1. *Nat Genet* 17:138–139, 1997
32. Horikawa Y, Iwasaki N, Hara M, Furuta H, Hinokio Y, Cockburn BN, Lindner T, Yamagata K, Ogata M, Tomonaga O, Kuroki H, Kasahara T, Iwamoto Y, Bell GI: Mutation in hepatocyte nuclear factor-1 beta gene (TCF2) associated with MODY. *Nat Genet* 17:384–385, 1997
33. Bell GI, Pilkis SJ, Weber IT, Polonsky KS: Glucokinase mutations, insulin secretion, and diabetes mellitus. *Ann. Rev Physiol* 58:171–186, 1996
34. Arden SD, Zahn T, Steegers S, Webb S, Bergman B, O'Brien RM, Hutton JC: Molecular cloning of a pancreatic islet specific glucose-6-phosphatase catalytic subunit-related protein. *Diabetes* 48:531–542, 1999
35. Tokuyama Y, Sturis J, DePaoli AM, Takeda J, Stoffel M, Tang J, Sun X, Polonsky KS, Bell GI: Evolution of β-cell dysfunction in the male Zucker diabetic fatty rat. *Diabetes* 44:1447–1457, 1995

36. Khan A, Chandramouli V, Ostenson CG, Low H, Landau BR, Efendic S: Glucose cycling in islets from healthy and diabetic rats. *Diabetes* 39:456–459, 1990
37. Khan A, Hong-Lie C, Landau BR: Glucose-6-phosphatase activity in islets from ob/ob and lean mice and the effect of dexamethasone. *Endocrinology* 136:1934–1938, 1995
38. Trinh K, Minassian C, Lange AJ, O'Doherty RM, Newgard CB: Adenovirus-mediated expression of the catalytic subunit of glucose-6-phosphatase in INS-1 cells. Effects on glucose cycling, glucose usage, and insulin secretion. *J Biol Chem* 272:24837–24842, 1997
39. Printz RL, Koch S, Potter LR, O'Doherty RM, Tiesinga JJ, Moritz S, Granner DK: Hexokinase II mRNA and gene structure, regulation by insulin, and evolution. *J Biol Chem* 268:5209–5219, 1993
40. Rowe L, Nadeau JH, Turner R, Frankel WN, Letts VA, Eppig JT, Ko MSH, Thurston SJ, Birkenmeier EH : Maps from two interspecific backcross DNA panels as a community mapping resource. *Mamm Genome* 5:253–274, 1994
41. Chirgwin JM, Przybyla AE, MacDonald RJ, Rutter WJ: Isolation of biologically active ribonucleic acid from sources enriched in ribonuclease. *Biochemistry* 18:5294–5299, 1979
42. Chrapkiewicz NB, Beale EG, Granner DK: Induction of the messenger ribonucleic acid coding for phosphoenolpyruvate carboxykinase in H4-II-E cells. Evidence for a nuclear effect of cyclic AMP. *J Biol Chem* 257:14428–14432, 1982
43. Sambrook J, Fritsch EF, Maniatis T: *Molecular Cloning: A Laboratory Manual*. 2nd Ed. Cold Spring Harbor, NY, Cold Spring Harbor Laboratory Press, 1989
44. Forest CD, O'Brien RM, Lucas PC, Magnuson MA, Granner DK: Regulation of phosphoenolpyruvate carboxykinase gene expression by insulin. Use of the stable transfection approach to locate an insulin responsive sequence. *Mol Endocrinol* 4:1302–1310, 1990
45. Jacoby DB, Zilz ND, Towle HC: Sequences within the 5′-flanking region of the S14 gene confer responsiveness to glucose in primary hepatocytes. *J Biol Chem* 264:17623–17626, 1989
46. O'Brien RM, Lucas PC, Yamasaki T, Noisin EL, Granner DK: Potential convergence of insulin and cAMP signal transduction systems at the phosphoenolpyruvate carboxykinase (PEPCK) gene promoter through C/EBP. *J Biol Chem* 269:30419–30428, 1994
47. O'Brien RM, Noisin EL, Suwanickul A, Yamasaki T, Lucas PC, Wang J-C, Powell DR, Granner DK: Hepatic nuclear factor-3 and hormone regulated expression of the PEPCK and IGFBP-1 genes. *Mol Cell Biol* 15:1747–1758, 1995
48. O'Brien RM, Halmi N, Printz RL, Granner DK: Structural and functional analysis of the human phosphoenolpyruvate carboxykinase gene promoter. *Biochem Biophys Acta* 1264:284–288, 1995
49. Jackson IJ: A reappraisal of non-consensus mRNA splice sites. *Nucleic Acids Res* 19:3795–3798, 1991
50. Haber BA, Chin S, Chuang E, Buikhuisen W, Naji A, Taub R: High levels of glucose-6-phosphatase gene and protein expression reflect an adaptive response in proliferating liver and diabetes. *J Clin Invest* 95:832–841, 1995
51 Lei KJ, Pan CJ, Shelly LL, Liu JL, Chou JY: Identification of mutations in the gene for glucose-6-phosphatase, the enzyme deficient in glycogen storage disease type 1a. *J Clin Invest* 93:1994–1999, 1994
52. Annabi B, Hiraiwa H, Mansfield BC, Lei KJ, Ubagai T, Polymeropoulos MH, Moses SW, Parvari R, Hershkovitz E, Mandel H, Fryman M, Chou JY: The gene for glycogen-storage disease type 1b maps to chromosome 11q23. *Am J Hum Genet* 62:400–405, 1998
53. Fenske CD, Jeffery S, Weber JL, Houlston RS, Leonard JV, Lee PJ: Localisation of the gene for glycogen storage disease type 1c by homozygosity mapping to 11q. *J Med Genet* 35:269–272, 1998
54. Lin B, Morris DW, Chou JY: The role of HNF1alpha, HNF3gamma, and cyclic AMP in glucose-6-phosphatase gene activation. *Biochemistry* 36:14096–14106, 1997
55. Shelton KD, Franklin AJ, Khoor A, Beechem J, Magnuson MA: Multiple elements in the upstream glucokinase promoter contribute to transcription in insulinoma cells. *Mol Cell Biol* 12:4578–4589, 1992
56. Sander M, German MS: The beta cell transcription factors and development of the pancreas. *J Mol Med* 75:327–340, 1997
57. Hussain MA, Lee J, Miller CP, Habener JF: POU domain transcription factor brain 4 confers pancreatic alpha-cell-specific expression of the proglucagon gene through interaction with a novel proximal promoter G1 element. *Mol Cell Biol* 17:7186–7194, 1997
58. Wang M, Drucker DJ: Activation of amylin gene transcription by LIM domain homeobox gene isl-1. *Mol Endocrinol* 10:243–251, 1996
59. Lange AJ, Argaud D, el-Maghrabi MR, Pan W, Maitra SR, Pilkis SJ: Isolation of a cDNA for the catalytic subunit of rat liver glucose-6-phosphatase: regulation of gene expression in FAO hepatoma cells by insulin, dexamethasone and cAMP. *Biochem Biophys Res Commun* 201:302–309, 1994
60. Massillon D, Chen W, Barzilai N, Prus-Wertheimer D, Hawkins M, Liu R, Taub R, Rossetti L: Carbon flux via the pentose phosphate pathway regulates the hepatic expression of the glucose-6-phosphatase and phosphoenolpyruvate carboxykinase genes in conscious rats. *J Biol Chem* 273:228–234, 1998
61. Argaud D, Kirby TL, Newgard CB, Lange AJ: Stimulation of glucose-6-phosphatase gene expression by glucose and fructose-2,6-bisphosphate. *J Biol Chem* 272:12854–12861, 1997
62. Massillon D, Barzilai N, Hawkins M, Prus-Wertheimer D, Rossetti L: Induction of hepatic glucose-6-phosphatase gene expression by lipid infusion. *Diabetes* 46:153–157, 1997
63. Chatelain F, Pegorier JP, Minassian C, Bruni N, Tarpin S, Girard J, Mithieux G: Development and regulation of glucose-6-phosphatase gene expression in rat liver, intestine, and kidney: in vivo and in vitro studies in cultured fetal hepatocytes. *Diabetes* 47:882–889, 1998
64. Metzger S, Goldschmidt N, Barash V, Peretz T, Drize O, Shilyansky J, Shiloni E, Chajek-Shaul T: Interleukin-6 secretion in mice is associated with reduced glucose-6-phosphatase and liver glycogen levels. *Am J Physiol* 273: E262–E267, 1997
65. Metzger S, Begleibter N, Barash V, Drize O, Peretz T, Shiloni E, Chajek-Shaul T: Tumor necrosis factor inhibits the transcriptional rate of glucose-6-phosphatase in vivo and in vitro. *Metabolism* 46:579–583, 1997
66. Magnuson MA: Glucokinase gene structure. Functional implications of molecular genetic studies. *Diabetes* 39:523–527, 1990
67. Pontoglio M, Sreenan S, Roe M, Pugh W, Ostrega D, Doyen A, Pick AJ, Baldwin A, Velho G, Froguel P, Levisetti M, Bonner-Weir S, Bell GI, Yaniv M, Polonsky KS: Defective insulin secretion in hepatocyte nuclear factor 1alpha-deficient mice. *J Clin Invest* 101:2215–2222, 1998
68. Pontoglio M, Barra J, Hadchouel M, Doyen A, Kress C, Bach JP, Babinet C, Yaniv M: Hepatocyte nuclear factor 1 inactivation results in hepatic dysfunction, phenylketonuria, and renal Fanconi syndrome. *Cell* 84:575–585, 1996
69. Lee YH, Sauer B, Gonzalez FJ: Laron dwarfism and non-insulin-dependent diabetes mellitus in the HNF-1α knockout mouse. *Mol Cell Biol* 18:3059–3068, 1998
70. Byrne MM, Sturis J, Menzel S, Yamagata K, Fajans SS, Dronsfield MJ, Bain SC, Hattersley AT, Velho G, Froguel P, Bell GI, Polonsky KS: Altered insulin secretory responses to glucose in diabetic and nondiabetic subjects with mutations in the diabetes susceptibility gene MODY3 on chromosome 12. *Diabetes* 45:1503–1510, 1996
71. De Vos A, Heimberg H, Quartier E, Huypens P, Bouwens L, Pipeleers D, Schuit F: Human and rat beta cells differ in glucose transporter but not in glucokinase gene expression. *J Clin Invest* 96:2489–2495, 1995